shown in Fig. 6. The regular graph Z_1 describes a space filling of E^3 by the two types of rhombohedra. This space filling has no translational subsymmetry from the cubic lattice in E^{12}.

Finally, we note that a translation shift in E_1^3 does not change Y_1 or Z_1 in their intrinsic structure. It follows that the 12-grid Y_1 and its dual Z_1 are determined by three real numbers.

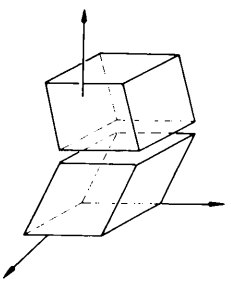

Fig. 6. Projection of the cubic 12-grid from E^{12} to E^3. The cells of the dual space filling are two different types of rhombohedra.

As mentioned before, the two types of rhombohedra were introduced by Mackay (1981) as the cells for a generalization of the patterns introduced by Penrose (1979) from two to three dimensions. What we believe is new in the present approach is the projection from E^{12} to E^3, the clear association with the icosahedral group $A(5)$, the introduction of the 12-grid and hexagrid in E^3, and the treatment of the orientation for the grid and its dual.

The present projection method opens the way towards the complete geometric analysis and classification of the hexagrids and their duals.

References

BRUIJN, N. G. DE (1981). *Ned. Akad. Weten. Proc. Ser. A*, **43**, 39–52, 53–66.

GROSSMAN, I. & MAGNUS, W. (1964). *Groups and Their Graphs*. New York: Random House.

KRAMER, P. (1982). *Acta Cryst.* **A38**, 257–264.

MACKAY, A. L. (1981). *Sov. Phys. Crystallogr.* **26**, 517–522.

PENROSE, R. (1979). *Math. Intell.* **2**, 32–37.

Acta Cryst. (1984). A**40**, 587–593

Shell Population and κ Refinements with Canonical and Density-Localized Scattering Factors in Analytical Form

BY ROB J. VAN DER WAL AND R. F. STEWART*

Department of Chemical Physics, University of Groningen, Nijenborgh 16, 9747 AG Groningen, The Netherlands

(*Received 9 December 1982; accepted 25 April 1984*)

Abstract

Scattering factors for outer shells of the first- and second-row series of atoms have been obtained by expansions with Jacobi functions. Both canonical and density-localized shell form factors have been studied. For κ refinements, both first and second derivatives are computed by analytical methods. Density-localized shell distributions differ from canonical shell distributions within a small sphere ($<0{\cdot}5$ Å) about the nucleus. Shell population and κ refinements on uracil at the monopole level give virtually identical results with canonical and density-localized form factors.

Introduction

In multipole analyses of electron density distributions from measured X-ray structure factors, the contraction or expansion of the atoms due to chemical bonding and redistribution of charge is often considered. For the monopole this can be partly achieved by keeping the density functions of the shells of a spherically averaged Hartree–Fock atom fixed, but with variable populations in the respective shells. Moreover, in κ refinements (Coppens, Guru Row, Stevens, Becker & Yang, 1979) the outermost shell of each atom can be contracted or expanded by rescaling K ($4\pi \sin\theta/\lambda$) as K/κ, with κ as a variable. For $\kappa > 1$ the shell density is contracted and for $\kappa < 1$ it is expanded. The results of shell populations and κ scaling may depend on the partitioning of the IAM (independent atom model) density into shells. The usual practice is to take atomic shell functions based on canonical Hartree–Fock atomic orbitals. In this case the valence-shell density on the nucleus is nonzero. As an example, for N(^4S) the valence density is $64{\cdot}4\ e\ Å^3$ compared to the core density of $1325{\cdot}5\ 3\ Å^3$ on the nucleus. One can seek a unitary transformation of the $1s$ and $2s$ canonical orbitals that minimizes the overlap of the $(1s')^2$ and $(2s')^2$

* Present address: Department of Chemistry, Carnegie-Mellon University, 4400 Fifth Avenue, Pittsburgh, PA 15213, USA

0108-7673/84/050587-07$01.50

densities (von Niessen, 1972). The resulting orbitals are called density-localized orbitals. In the case of N(^4S), the valence density is reduced to 0·8 e Å^3 on the nucleus and the core density is increased to 1389·1 e Å^3. We note that such unitary transformations preserve the overall atomic density. In the present paper we will compare the canonical shell form factors with localized ones. Spin-restricted Hartree–Fock orbitals have been localized as if they were spin unrestricted and only orbitals of the *same* angular momentum have been density localized among themselves (Stewart, 1980).

Clementi (1965) has tabulated spin-restricted Hartree–Fock orbitals for the neutral atoms up through Kr. These orbitals are spanned by Slater-type functions, so that both electron densities and form factors can be easily expressed in analytical form. The Clementi wavefunctions give atomic form factors for the first- and second-row atoms that are in close agreement with the numerical results of Cromer & Waber (1974). We have generated density-localized orbitals from Clementi's compilation, so that the local shell form factors are spanned by the same density basis functions. Thus first and second derivatives of the shell form factors with respect to κ can be evaluated analytically for all $\sin\theta/\lambda$ values in an X-ray structure-factor analysis. The number of radial-density basis functions, per atom, is rather large, however. A typical first-row atom, such as N(^4S), has 31 functions and for a second-row atom, such as Si(^3P), the number is 72. For actual application to a set of measured X-ray structure-factor amplitudes, computation of these analytical form factors demands an unwarrantable amount of CPU time. A second objective in the present research is to seek a rather smaller set of analytical functions which can reproduce the shell form factors, as well as the first and second derivatives with respect to the scaling parameter, κ, to four-decimal-place accuracy.

Analytical representation of shell densities and form factors

At large r an atomic density has the asymptotic form $\exp(-\gamma r)$. At small r, centered on a nucleus which is treated as a source point, the electron density varies as r^l where l is the order of a multipole. For example, the ^3P state for C has a quadrupole component ($l=2$) in its charge density. We take $r^l\exp(-\gamma r)$ as a starting point and seek a complete set of functions on the interval $0\le r\le\infty$. An appropriate set is spanned by the Laguerre polynomials, $L_n^{(2l+2)}(2\gamma r)$. We thus use the expansion

$$\rho_l(r)\sim r^l e^{-\gamma r}\sum_{n=0} a_n L_n^{(2l+2)}(2\gamma r). \qquad (1)$$

The corresponding Fourier–Bessel transform, derived in the Appendix, is

$$f_l(K)\sim(K/\gamma)^l\gamma^{-(l+3)}[1+(K/\gamma)^2]^{-(l+2)} \times\sum_n 2^n a_n(n+2l+2)! \times P_n^{(l+3/2,l+1/2)}(t)/(2n+2l+1)!!, \qquad (2)$$

where $P_n^{(\alpha,\beta)}(t)$ is a Jacobi polynomial and

$$t=[(K/\gamma)^2-1]/[(K/\gamma)^2+1]. \qquad (3)$$

For the present task of representing spherical-shell form factors, we take $l=0$. The Laguerre functions in (1) comprise the sequence $\{g_n\}$, where

$$g_n=e^{-\gamma r}L_n^{(2)}(2\gamma r), \qquad (4)$$

so that we obtain

$$\rho_{\rm shell}(r)\sim\rho^c_{\rm shell}=\sum_n a_n g_n. \qquad (5)$$

The Fourier coefficients corresponding with the orthogonal set of functions in (5) are calculated as

$$a_n=[(2\gamma)^3 n!/(n+2)!]\int_0^\infty \rho_{\rm shell}g_n r^2\,{\rm d}r. \qquad (6)$$

for an appropriate choice of γ the coefficients, (6), give, when substituted in (5), the best mean-square approximation to $\rho_{\rm shell}(r)$. A consequence of the Fourier integral theorem is that the form factor, obtained from (5) and (6), is the best mean-square fit to the atomic shell form factor as well. The nonlinear parameter γ can be found by a grid search until

$$\varepsilon=\int_0^\infty[\rho_{\rm shell}-\sum_n a_n g_n]^2 r^2\,{\rm d}r \qquad (7)$$

is a minimum, at which point

$$\sum_n a_n\int_0^\infty\rho_{\rm shell}(\partial g_n/\partial\gamma)r^2\,{\rm d}r =\sum_n\sum_{n'}a_n a_{n'}\int_0^\infty g_n(\partial g_{n'}/\partial\gamma)r^2\,{\rm d}r. \qquad (8)$$

Equations (6) and (8) are the formal solution to the expansion. The shell density functions can be simply represented from the Clementi (1965) basis functions as

$$\rho_{\rm shell}(r)=\sum_k D_k r^{N_k-2}\exp(-\alpha_k r), \qquad (9)$$

where

$$\int_0^\infty\rho_{\rm shell}(r)r^2\,{\rm d}r=1 \qquad (10)$$

and $\{D_k\}$ may describe either a canonical or a localized shell. With (9) substituted into (6) and (8), all integrals can be evaluated by standard methods. Although (6) and (8) are the best mean-square fit to $\rho_{\rm shell}$, other solutions were considered whereby constraints were imposed on $\rho^c_{\rm shell}$. Each constraint

degrades the quality of the mean-square fit. After some experimentation, it was decided to impose normalization [(10)] on ρ^c_{shell}. For this case we modify (6),

$$a_n = (2\gamma)^3\left\{ n!G_n/(n+2)! + (-3)^{n+1} \times\left[\sum_{k=0}^{N}(-1)^k G_k - \tfrac{1}{8}\right]\Big/(N+3)(N+2)(N+1)\right\} \tag{11}$$

and

$$G_n = \int_0^\infty \rho_{\text{shell}} g_n r^2\, dr. \tag{12}$$

In (11), N is the maximum order of the orthogonal function used in (5). Also note that as N gets large (11) collapses to (6).

Equations (8) and (11) were solved for both canonical and localized outer-shell density functions for the neutral atoms Li to Cl for increasing values of N until five- to four-digit accuracy in representing the shell form factor was achieved. For the first-row atoms, the first thirteen Laguerre functions (4) ($N = 12$) were needed for the canonical L shells, while $N = 8$ was adequate for the localized L shells. The M shells for the second-row atoms were fitted with N equal to 19 and 11 for the canonical and localized densities, respectively.

The shell form factor, corresponding to (5), follows from (2) with $l = 0$:

$$f^c_{\text{shell}}(K) = \gamma^{-3}[1+(K/\gamma)^2]^{-2} \times \sum_{n=0}^{N} 2^n a_n (n+2)! P_n^{(3/2,1/2)}(t)/(2n+1)!! \tag{13}$$

Recursion relations for the Jacobi polynomials, $P_b^{(3/2,1/2)}(t)$, allow rapid evaluation of (13). We first multiply the a_n by $2/\gamma^3$ and relabel them b_n. We need now to express (13) as

$$f^c_{\text{shell}}(K) = \sum_{n=0}^{N} b_n H_n(K, \gamma), \tag{14}$$

where H_n obeys the recursion

$$H_{n+1} = \{[1+(n+2)(n+1)2t]H_n - (n+2)^2 H_{n-1}\}/(n+1)^2 \tag{15}$$

with

$$H_0 = [1+(K/\gamma)^2]^{-2} \tag{16}$$

$$H_1 = [1+4t]H_0 \tag{17}$$

and t is given by (3). In most crystallographic programs the scattering variable is usually computed as $\sin\theta/\lambda$ (Å^{-1}), which can take the place of $K = 4\pi \sin\theta/\lambda$ (a.u.) in (16) if γ is rescaled by $(4\pi a_0)^{-1}$ where a_0, the Bohr radius, is 0·529177 Å. The parameters b_n and $\gamma/(4\pi a_0)$ for the canonical outer shells of the neutral first- and second-row atoms are given in Table 1.

For the corresponding inner shells, similar expansions for the atoms Li(^1S) to Cl(^2P) are tabulated in Table 2.* The table does not include Ne(^1S). Note that the expansion lengths are rather smaller than for comparable quality of fit to the outer (L and M) shells of the first- and second-row atoms, respectively.

In a κ refinement, it is necessary to compute both the first and second derivatives of $f^c_{\text{shell}}(K/\kappa)$ with respect to κ. We implement this in the same way as shown with (14)–(17).

$$\partial f^c_{\text{shell}}/\partial\kappa = \sum_{n=0}^{N} b_n H'_n \tag{18}$$

$$\partial^2 f^c_{\text{shell}}/\partial\kappa^2 = \sum_{n=0}^{N} b_n H''_n, \tag{18'}$$

where the recursions for H'_n and H''_n are

$$H'_{n+1} = (2\kappa)^{-1}\{[3n+4+(n+1)(n+2)2t]H_n - (n+2)(2n+3)H_{n-1}\}/(n+1) \tag{19}$$

$$H''_{n+1} = (2\kappa)^{-1}(n+2)\{[1+(n+1)2t]H'_n - (2n+3)H'_{n-1} - 4(n+1)(1-t^2)H_n/(2\kappa)\}/(n+1). \tag{19'}$$

The starting values for (19) and (19′) are

$$H'_0 = 2(1+t)H_0/\kappa \tag{20}$$

$$H'_1 = [3(2t)^2+5(2t)-2]H_0/\kappa \tag{21}$$

$$H''_0 = 6t(1+t)H_0/(\kappa)^2 \tag{20'}$$

$$H''_1 = 6(8t^3+7t^2-3t-2)H_0/(\kappa)^2. \tag{21'}$$

Although the expressions in (14)–(21′) may seem cumbersome, they have been easily coded into a 42-line Fortran program which rapidly evaluates the shell form factor as well as its first and second derivatives with respect to the scaling parameter κ. The first and second derivatives (18) and (18′) with $0{\cdot}75 \le \kappa \le 1{\cdot}25$ for the N values cited above were found to agree with the corresponding derivatives of the Clementi shell form factors to within four-digit accuracy.

We emphasize that our analytical expansions are over the full radial interval from zero to infinity. This means the analytical form factors have the same mean-square quality over all of K space. With a population parameter and γ scaled by κ, one can use (4) and (5) to represent the density distribution or to compute some average property, such as $\langle r^{-1}\rangle$. In practice, one is limited to measurements in a restricted K space so that parameters such as monopole populations and κ's suffer from series termination of the data. The $f^c_{\text{shell}}(K)$ in (13) or (14), however, is the

* We have included these results at the request of a referee. The inner-shell values tabulated by Cromer & Waber (1974) are virtually the same as the results that can be generated from Table 2.

Table 1. *Jacobi fits to canonical L-shell and M-shell scattering factors for first- and second-row atoms, respectively*

	Li	Be	B	C	N	O	F
$\gamma/4\pi a_0$	0·3697066	0·5039780	0·5932428	0·6997227	0·8094559	0·8967804	0·9817579
b_0	0·623102E−01	0·840349E−01	0·102840E+00	0·117180E+00	0·128774E+00	0·144853E+00	0·160690E+00
b_1	−0·117258E−01	−0·142182E−01	−0·388805E−01	−0·554723E−01	−0·672132E−01	−0·782452E−01	−0·878395E−01
b_2	0·501891E−01	0·615731E−01	0·658595E−01	0·640755E−01	0·615500E−01	0·594930E−01	0·571926E−01
b_3	−0·202230E−01	−0·180013E−01	−0·136407E−01	−0·116474E−01	−0·105081E−01	−0·823943E−02	−0·650647E−02
b_4	0·127891E−01	0·111664E−01	0·923874E−02	0·823507E−02	0·756087E−02	0·716584E−02	0·689202E−02
b_5	−0·434302E−02	−0·315125E−02	−0·201568E−02	−0·166836E−02	−0·148389E−02	−0·119324E−02	−0·913551E−03
b_6	0·230885E−02	0·184752E−02	0·145126E−02	0·124586E−02	0·111808E−02	0·107280E−02	0·102626E−02
b_7	−0·680884E−03	−0·469039E−03	−0·280612E−03	−0·216382E−03	−0·194723E−03	−0·161363E−03	−0·118918E−03
b_8	0·371597E−03	0·301664E−03	0·246107E−03	0·206320E−03	0·180306E−03	0·184067E−03	0·178207E−03
b_9	−0·872610E−04	−0·608809E−04	−0·365107E−04	−0·263422E−04	−0·240351E−04	−0·203947E−04	−0·144906E−04
b_{10}	0·583690E−04	0·503577E−04	0·457293E−04	0·382433E−04	0·317781E−04	0·354894E−04	0·349569E−04
b_{11}	−0·854558E−05	−0·625804E−05	−0·420349E−05	−0·301365E−05	−0·263325E−05	−0·250369E−05	−0·187914E−05
b_{12}	0·998906E−05	0·918548E−05	0·964819E−05	0·821415E−05	0·632996E−05	0·795362E−05	0·791170E−05
	Na	Mg	Al	Si	P	S	Cl
$\gamma/4\pi a_0$	0·5648452	0·6880977	0·7308943	0·8253179	0·9193719	0·9889269	1·0672503
b_0	0·163266E−01	0·231399E−01	0·314483E−01	0·364808E−01	0·408794E−01	0·462700E−01	0·506007E−01
b_1	−0·273806E−02	−0·356667E−02	−0·435803E−02	−0·455265E−02	−0·488458E−02	−0·531348E−02	−0·569278E−02
b_2	0·603966E−02	0·732173E−02	0·950551E−02	0·921327E−02	0·908231E−02	0·101322E−01	0·107216E−01
b_3	−0·840895E−02	−0·873265E−02	−0·126463E−01	−0·136578E−01	−0·148128E−01	−0·170545E−01	−0·186537E−01
b_4	0·110746E−01	0·139140E−01	0·152070E−01	0·154220E−01	0·156680E−01	0·159235E−01	0·160152E−01
b_5	−0·526377E−02	−0·508977E−02	0·480753E−02	−0·522659E−02	−0·558213E−02	−0·542847E−02	−0·536704E−02
b_6	0·605125E−02	0·640668E−02	0·608918E−02	0·583259E−02	0·558617E−02	0·526468E−02	0·500402E−02
b_7	−0·237965E−02	−0·201227E−02	−0·139511E−02	−0·153810E−02	−0·159619E−02	−0·141108E−02	−0·132378E−02
b_8	0·255451E−02	0·236469E−02	0·210194E−02	0·189949E−02	0·171900E−02	0·155999E−02	0·143445E−02
b_9	−0·899115E−03	−0·685644E−03	−0·410287E−03	−0·442425E−03	−0·441676E−03	−0·367447E−03	−0·334335E−03
b_{10}	0·966976E−03	0·811298E−03	0·722128E−03	0·617515E−03	0·529644E−03	0·473934E−03	0·427802E−03
b_{11}	−0·305198E−03	−0·218131E−03	−0·126207E−03	−0·132947E−03	−0·125764E−03	−0·103456E−03	−0·927566E−04
b_{12}	0·349164E−03	0·272711E−03	0·252499E−03	0·201840E−03	0·162399E−03	0·143702E−03	0·126662E−03
b_{13}	−0·946831E−04	−0·651375E−04	−0·384677E−04	−0·390406E−04	−0·345737E−04	−0·289185E−04	−0·257653E−04
b_{14}	0·124118E−03	0·917465E−04	0·903732E−04	0·663898E−04	0·497114E−04	0·435753E−04	0·373048E−04
b_{15}	−0·263991E−04	−0·177200E−04	−0·111540E−04	−0·105159E−04	−0·861004E−05	−0·737057E−05	−0·652120E−05
b_{16}	0·446796E−04	0·315449E−04	0·334712E−04	0·224577E−04	0·157103E−04	0·137066E−04	0·114413E−04
b_{17}	−0·632753E−05	−0·415834E−05	−0·315988E−05	−0·255165E−05	−0·189300E−05	−0·165138E−05	−0·143863E−05
b_{18}	0·169637E−04	0·115026E−04	0·131559E−04	0·820455E−05	0·546744E−05	0·477748E−05	0·394513E−05

Table 2. *Jacobi fits to canonical K-shell scattering factors for first-row atoms and (K + L)-shell scattering factors for second-row atoms*

	Li	Be	B	C	N	O	F
$\gamma/4\pi a_0$	0·9109680	1·2457784	1·5544170	1·8480643	2·1456420	2·4754691	2·7495894
b_0	0·830834E+00	0·834171E+00	0·857171E+00	0·883023E+00	0·899094E+00	0·893033E+00	0·916171E+00
b_1	−0·368101E−01	−0·394609E−01	−0·350738E−01	−0·289049E−01	−0·249865E−01	−0·272591E−01	−0·208436E−01
b_2	0·887124E−02	0·722628E−02	0·583116E−02	0·483268E−02	0·416351E−02	0·396757E−02	0·343730E−02
b_3	−0·331007E−03	−0·270201E−03	−0·159879E−03	−0·413995E−04	−0·186525E−04	−0·539375E−04	0·944206E−05
b_4	0·144318E−03	0·915130E−04	0·670809E−04	0·557327E−04	0·508778E−04	0·553951E−04	0·503049E−04
b_5	−0·158351E−05	−0·662926E−06	−0·733034E−06	−0·775820E−06	−0·728544E−06	−0·648773E−06	−0·681676E−06
	Na	Mg	Al	Si	P	S	Cl
$\gamma/4\pi a_0$	1·5048029	1·7106067	1·9199764	2·1147912	2·3115451	2·4970875	2·6543019
b_0	0·589068E+00	0·571202E+00	0·555558E+00	0·547378E+00	0·539896E+00	0·536544E+00	0·540948E+00
b_1	0·127307E+00	0·112152E+00	0·998416E−01	0·916561E−01	0·847283E−01	0·799250E−01	0·781051E−01
b_2	0·106611E+00	0·989946E−01	0·927784E−01	0·894370E−01	0·865359E−01	0·850564E−01	0·859808E−01
b_3	0·123412E−01	0·767207E−02	0·407857E−02	0·207861E−02	0·423988E−03	−0·477662E−03	−0·171178E−03
b_4	0·150475E−01	0·130900E−01	0·116828E−01	0·107981E−01	0·100982E−01	0·959603E−02	0·931638E−02
b_5	0·146060E−02	0·699336E−03	0·156812E−03	−0·640212E−04	−0·236396E−03	−0·282987E−03	−0·115670E−03
b_6	0·234534E−02	0·187960E−02	0·155544E−02	0·135125E−02	0·119340E−02	0·107911E−02	0·997710E−03
b_7	0·184539E−03	0·734710E−04	0·321484E−05	−0·153090E−04	−0·306003E−04	−0·272725E−04	0·497100E−05
b_8	0·395515E−03	0·286441E−03	0·219441E−03	0·176898E−03	0·147404E−03	0·125906E−03	0·110793E−03
b_9	0·243351E−04	0·921464E−05	−0·487574E−06	−0·933938E−06	−0·260401E−05	−0·155604E−05	0·324336E−05
b_{10}	0·714563E−04	0·470884E−04	0·331910E−04	0·247941E−04	0·193431E−04	0·158873E−04	0·134109E−04
b_{11}	0·317627E−05	0·108682E−05	−0·558051E−07	0·148754E−06	−0·561664E−07	0·324638E−07	0·604090E−06
b_{12}	0·138932E−04	0·836999E−05	0·533522E−05	0·375570E−05	0·272950E−05	0·218516E−05	0·180897E−05
b_{13}	0·199094E−06	0·356704E−07	−0·135316E−07	0·294927E−07	0·326781E−09	0·104572E−07	0·560124E−07
b_{14}	0·299916E−05	0·163823E−05	0·935430E−06	0·642196E−06	0·445329E−06	0·344088E−06	0·290276E−06

Fourier–Bessel transform of $\rho^c_{\text{shell}}(r)$ in (5), and one may convert the functions from one space to another with no series termination. Our construction here of an analytical form factor is in contrast to fits over *finite* segments of K space (*e.g.* Cromer & Mann, 1968). For the latter case, the analytical functions cannot have a reliable Fourier–Bessel transform to r space.

Comparison of canonical to localized shell radial functions and form factors

It is instructive to observe how the density localization procedure redistributes the canonical shell density into the localized shell. For the L-shell functions of $C(^3P)$, $N(^4S)$ and $O(^3P)$,

$$\rho^{\text{can}}_L(r) = 2|\chi_{2s}|^2 + n|\chi_{2p}|^2 \qquad (22)$$

and

$$\rho_L^{\rm loc}(r) = 2|\chi_{os}|^2 + n|\chi_{2p}|^2 \qquad (22')$$

and n is 2, 3 or 4 for C, N or O. The χ_{os} is the localized outer s orbital and χ_{2s} is the canonical $2s$ atomic orbital. Fig. 1 is a display of the difference,

$$\Delta\rho_L = |\chi_{2s}|^2 - |\chi_{os}|^2 \qquad (23)$$

as a function of r for C, N and O. Each orbital has unit norm. The values at r equal to zero (not displayed in Fig. 1) are 18·5, 31·8 and 50·9 e Å^{-3} for C, N and O, respectively. Nodes occur near 0·12, 0·14, and 0·16 Å for the O, N, and C atoms, respectively, and reach minima near r equal to 0·17, 0·20, and 0·23 Å. We see that by localization the charge density within a sphere of ~0·14 Å from the nucleus is redistributed into a shell that extends out to about 0·5 Å. The corresponding localized K shell becomes more concentrated in charge density within 0·14 Å of the nucleus.

The difference radial form factors for the difference functions in (23),

$$\Delta f_L(\mathrm{K}) = \int_0^\infty \Delta\rho_L(r) j_0(Kr) r^2\, dr, \qquad (24)$$

are plotted in Fig. 2 as a function of sin θ/λ (Å^{-1}) for the atoms C, N and O. The localized L-shell form factors have larger amplitude by ~0·01 within 0·2 to 0·5 Å^{-1} in sin θ/λ; the canonical shell amplitudes are larger by ~0·02 in the high sin θ/λ region of 1·0 to 1·4 Å^{-1}. It is in this domain where the Fourier–Bessel components of the charge density differences (displayed in Fig. 1) within ~0·15 Å of the nucleus are largest. The magnitude of the differences in these shell form factors is rather small. For diffraction data restricted to a sphere within 0·9 Å^{-1} in sin θ/λ, one would expect similar results in κ variation of either shell form factor. Only with a large data set and very small amplitude of atomic motion do we anticipate a significantly different set of κ and population parameters among the two L-shell form factors.

Application to uracil

Monopole analyses have previously been applied to uracil (Stewart, 1970; Yãnez & Stewart, 1978). The structure-factor amplitudes, $|F_{\rm H}|$, and corresponding weights, $w_{\rm H}$, were taken from Stewart & Jensen (1967). The diffraction data were measured at room temperature with a manual diffractometer. A full hemisphere was measured up to sin $\theta/\lambda = 0{\cdot}6$ Å^{-1}; other data were collected out to 0·9 Å^{-1}, but only for those reflections for which net counts were calculated to be larger than 200. Altogether, 1163 unique reflections constitute the data set for a least-squares refinement. A conventional structure refinement (89 parameters), based on $|F_{\rm H}|$, had a final $R_w = 0{\cdot}037$* (Stewart & Jensen, 1967, 1969).

We choose the final refined model of the atomic parameters as a fixed reference point for an L-shell projection analysis. The analytical L-shell (localized or canonical) form factors for C, N and O with the corresponding localized or canonical K-shell form factors were used. For the hydrogen atoms, a form factor derived from a $1s$ Slater-type function with an exponent of 1·24 Bohr^{-1} was used. A conventional refinement with atomic shell populations fixed at the neutral-atom values was in virtual agreement with the earlier results reported by Stewart & Jensen (1967)

* $R_w = \{\sum_{\rm H} w_{\rm H}(|F_{\rm H}| - |F_{\rm H}^c|)^2 / \sum_{\rm H} w_{\rm H}|F_{\rm H}|^2\}^{1/2}$.

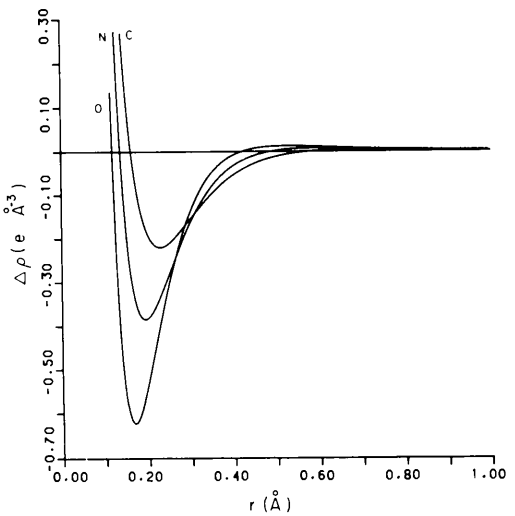

Fig. 1. Plot of $\Delta\rho$ (e Å^{-3})[(23)] *versus* r (Å) for atoms C, N and O. Values of $\Delta\rho$ at $r = 0$ are 18·5, 31·8 and 50·9 e Å^{-3} for C, N and O, respectively.

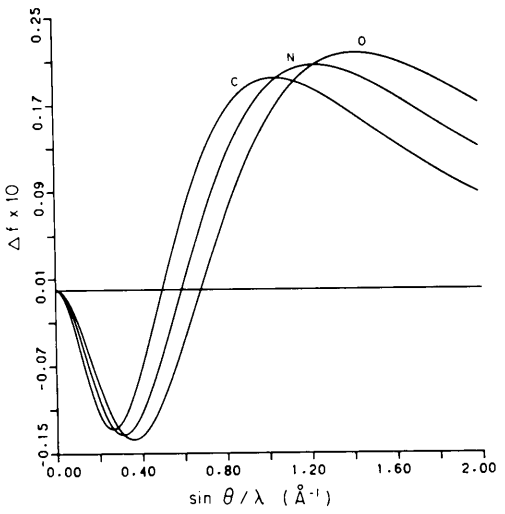

Fig. 2. Plot of $\Delta f \times 10$ [(24)] *versus* sin θ/λ (Å^{-1}) for atoms C, N and O.

with the exception of hydrogen-atom (isotropic) thermal parameters. The analytical 1*s* form factor for H in the present study gives rise to thermal parameters which are ~40% larger than the earlier work where a numerical form factor for H bonded in H_2 (Stewart, Davidson & Simpson, 1965) was used. With the atomic and thermal parameters fixed at the conventional results, the *L*-shell form factors and H-atom form factors were assigned variable monopole electron populations for each atom; the *K*-shell monopole populations were constrained to be two for all non-hydrogen atoms. In addition to the monopole population parameters, κ were varied for the *L* shells. Altogether, 20 parameters were refined. The quantity minimized was $\sum_{\mathbf{H}} w_{\mathbf{H}}(|F_{\mathbf{H}}| - |F^c_{\mathbf{H}}|)^2$. The least-squares matrix was constructed with explicit second-derivative terms. A summary of the refinement results with canonical shells is given in Table 3. Identical results were found with localized shells as well. The final R_w, with our restricted model, is 0·034.

It is somewhat interesting to compare the κ refined values with an earlier *L*-shell result whereby the canonical shell form factors were fixed at κ of unity (Stewart, 1970). The oxygen *L* shells are scaled by $\kappa \sim 0{\cdot}97$; this 3% expansion in the density function leads to a net charge of $\sim -0{\cdot}27$, whereas the previous analysis revealed a net charge of zero. For the nitrogen atoms the net charge is $\sim -0{\cdot}09$ with $\kappa \sim 0{\cdot}99$, whereas for κ unity the net charge was +0·05. Except for C(5), the carbon atoms are contracted by 3% and show a positive net charge of +0·3 to +0·2. In the case of C(5) the shell density is expanded by 1% and has a negative net charge of 0·3. For the results with an unscaled canonical *L*-shell form factor, the carbon atoms were virtually neutral except for C(5) which had a net charge of −0·2. The results we have here with variable κ scaling are rather similar to the *L*-shell projection values with standard molecular *L*-shell (nodeless density functions) form factors (Stewart, 1970). It is also evident from Table 3 that contracted *L*-shell density functions have net positive charge, while expanded functions contain net negative charge.

At completion of the *L*-shell projection refinements, a stationary point was achieved and the correlation coefficients were determined from the inverse least-squares matrix elements. The *L*-shell population coefficients and the corresponding κ parameters were always negatively correlated for the same atom. The values given in Table 3 vary from −0·90 to −0·85. This is an expected result which serves to emphasize that a variance calculation for an electrostatic property, such as the molecular dipole moment or total electrostatic potential, derived from the model density in Table 3, must include the covariance terms for a meaningful estimated standard deviation. All other correlation coefficients among the twenty parameters were less than 0·707 and greater than −0·707.

Table 3. *Results of a κ refinement on uracil*

q is the net atomic charge for the last decimal place. E.s.d.'s are shown in ( ) for the last decimal place. Cmκ is the correlation coefficient between κ and the *L*-shell monopole population.

Atom	*q*	κ	Cmκ
O(7)	−0·28 (6)	0·968 (6)	−0·8697
O(8)	−0·25 (6)	0·973 (6)	−0·8888
N(1)	−0·11 (7)	0·987 (7)	−0·9009
N(3)	−0·07 (7)	0·994 (7)	−0·8889
C(2)	0·32 (8)	1·03 (1)	−0·8861
C(4)	0·33 (8)	1·03 (1)	−0·8739
C(5)	−0·34 (9)	0·987 (9)	−0·8542
C(6)	0·22 (9)	1·02 (1)	−0·9024
H(9)	0·07 (3)	—	—
H(10)	−0·01 (3)	—	—
H(11)	0·05 (3)	—	—
H(12)	0·07 (3)	—	—

The κ refinements of either localized on canonical shells are virtually identical based on the data for crystalline uracil. The only advantage in the analytical localized shell form factors is a slight gain in computation time due to the smaller expansion (nine functions) compared to the canonical expansion (13 functions). This is not a rate-determining step, however, in the construction of the least-squares matrix.

The sample calculation in application to uracil is a model restricted to *L*-shell projections. Rather more extensive refinements by van der Wal (1982) have been pursued, but the restricted data set for uracil precludes a definitive result for the static electron density.

Support from the Netherlands Organization for the Advancement of Pure Research (ZWO) and by the National Science Foundation Grant CHE-80-16165 is gratefully acknowledged. We thank Professor Vos for her interest in and support of this work. Computations were carried out at the computing center of the University of Groningen and by the Chemistry VAX at Carnegie–Mellon University.

APPENDIX

Fourier–Bessel transform of $r^l e^{-\gamma r} L_n^{(2l+2)}(2\gamma r)$

For radial multipoles spanned by the functions $r^l L_n^{2l+2}(2\gamma r)\, e^{-\gamma r}$ the corresponding radial form factor is

$$f_{n,l}(K) = \int_0^\infty r^{l+2}\, e^{-\gamma r} L_n^{(2l+2)}(2\gamma r) j_l(Kr)\, \mathrm{d}r, \qquad (A1)$$

where K is $4\pi \sin\theta/\lambda$. The evaluation of (*A*1) closely follows the method used by Podolsky & Pauling (1929). We define

$$F = \sum_{n=0}^{\infty} f_{n,l} Z^n \quad |Z| < 1. \qquad (A2)$$

The generating function for a Laguerre polynomial

(*Handbook of Mathematical Functions*, 1972, equation 22.9.15),

$$(1-Z)^{-\alpha-1}\exp[-XZ/(1-Z)]=\sum_{n=0}^{\infty}L_n^{\alpha}(X)Z^n, \quad (A3)$$

can be used with (*A*1) to rewrite (*A*2) as

$$F=\sum_{n=0}^{\infty}\left\{\int_0^{\infty}r^{l+2}\exp[-\gamma r(1+Z)/(1-Z)]j_l(Kr)\,dr\right\}\times Z^n/(1-Z)^{2l+3}. \quad (A4)$$

The integral in (*A*4) may be evaluated in simple closed form [Epstein & Stewart, 1977, equation (*A*2)]. With some algebraic rearrangements,

$$F=\frac{(2l+2)!(K/\gamma)^l}{(2l+1)!!\gamma^{l+3}[1+(K/\gamma)^2]^{l+2}}\times\sum_{n=0}^{\infty}\frac{(1+Z)}{(1-2tZ+Z^2)^{l+2}}Z^n, \quad (A5)$$

where

$$t=[(K/\gamma)^2-1]/[(K/\gamma)^2+1]. \quad (A6)$$

From the generating function for a Gegenbauer polynomial (*Handbook of Mathematical Functions*, 1972, equation 22.9.3), we can write (*A*5) as

$$F=\frac{(2l+2)!(K/\gamma)^l}{(2l+1)!!\gamma^{l+3}[1+(K/\gamma)^2]^{l+2}}\times\sum_{n=0}^{\infty}[C_n^{(l+2)}(t)+C_{n-1}^{(l+2)}(t)]Z^n. \quad (A7)$$

The Gegenbauer polynomial, $C_n^{(l+2)}(t)$, may be expressed as a Jacobi polynomial, $P_n^{(l+3/2,l+3/2)}(t)$ (*Handbook of Mathematical Functions*, 1972, equation 22.5.20). The sum of the two polynomials in (*A*7) then satisfies a recurrence relation for Jacobi polynomials (*Handbook of Mathematical Functions*, 1972, equation 22.7.19). Thus (*A*7) can be simplified to

$$F=(K/\gamma)^l\gamma^{-(l+3)}[1+(K/\gamma)^2]^{-(l+2)}\times\sum_{n=0}^{\infty}\frac{2^n(n+2l+2)!}{(2n+2l+1)!!}P_n^{(l+3/2,l+1/2)}(t)Z^n. \quad (A8)$$

In comparing (*A*2) to (*A*8), we have the desired result,

$$f_{n,l}(K)=\frac{(K/\gamma)^l 2^n(n+2l+2)!}{\gamma^{l+3}[1+(K/\gamma)^2]^{l+2}(2n+2l+1)!!}\times P_n^{(l+3/2,l+1/2)}(t). \quad (A9)$$

References

CLEMENTI, E. (1965). *IBM J. Res. Dev.* **9**, Suppl. 2.

COPPENS, P., GURU ROW, T. N., STEVENS, E. D., BECKER, P. J. & YANG, Y. W. (1979). *Acta Cryst.* A**35**, 63–72.

CROMER, D. T. & MANN, J. B. (1968). *Acta Cryst.* A**24**, 321–324.

CROMER, D. T. & WABER, J. T. (1974). *International Tables for X-ray Crystallography*, Vol. IV, pp. 71–145. Birmingham: Kynoch Press.

EPSTEIN, J. & STEWART, R. F. (1977). *J. Chem. Phys.* **66**, 4057–4064.

Handbook of Mathematical Functions (1972). Edited by M. ABRAMOWITZ & I. A. STEGUN. *Nat. Bur. Stand. Appl. Math. Ser.* No. 55. US Government Printing Office, Washington, DC 20402.

NIESSEN, W. VON (1972). *J. Chem. Phys.* **56**, 4290–4297.

PODOLSKY, B. & PAULING, L. (1929). *Phys. Rev.* **34**, 109–116.

STEWART, R. F. (1970). *J. Chem. Phys.* **53**, 205–213.

STEWART, R. F. (1980). In *Electron and Magnetization Densities in Molecules and Crystals*, edited by P. BECKER, pp. 427–431. New York: Plenum Press.

STEWART, R. F., DAVIDSON, E. R. & SIMPSON, W. T. (1965). *J. Chem. Phys.* **42**, 3175–3187.

STEWART, R. F. & JENSEN, L. H. (1967). *Acta Cryst.* **23**, 1102–1105.

STEWART, R. F. & JENSEN, L. H. (1969). *Z. Kristallogr.* **128**, 133–147.

WAL, R. J. VAN DER (1982). Thesis, Univ. of Groningen.

YÁNEZ, M. & STEWART, R. F. (1978). *Acta Cryst.* A**34**, 648–651.

Acta Cryst. (1984). A**40**, 593–600

The Implications of Normalizers on Group–Subgroup Relations Between Space Groups

BY ELKE KOCH

Institut für Mineralogie, Lahnberge, D-3550 Marburg, Federal Republic of Germany

(*Received* 19 *December* 1983; *accepted* 26 *April* 1984)

Abstract

A hierarchy of classifications for subgroups of space groups by means of Euclidean and affine normalizers is introduced. The different levels of this classification scheme are illustrated in detail with examples and its usefulness for various problems is demonstrated. The Euclidean (or affine) normalizers of a space group G and of one of its subgroups U may either coincide [$N(G)=N(U)$], or form a group–subgroup pair [$N(G)\supset N(U)$ or $N(G)\subset N(U)$], or share only a common subgroup [$N(G)\not\supset N(U)$ and $N(G)\not\subset N(U)$]. The different implications of these cases on the equivalence classes of subgroups (or supergroups)

0108-7673/84/050593-08$01.50